Temporal variation of light availability in coastal benthic habitats: Effects of clouds, turbidity, and tides

Kenneth R. N. Anthony[1]

Centre for Coral Reef Biodiversity, School of Marine Biology and Aquaculture, James Cook University, Townsville, Queensland 4811, Australia

Peter V. Ridd

Marine Geophysical Laboratory, School of Mathematics and Physical Sciences, James Cook University, Townsville, Queensland 4811, Australia

Alan R. Orpin

National Institute of Water and Atmospheric Research (NIWA), Private Bag 14-901, Kilbirnie, Wellington, New Zealand

Piers Larcombe

Centre for Environment, Fisheries, and Aquaculture Science (CEFAS), Pakefield Road, Lowestoft, Suffolk NR33 0HT, Great Britain

Janice Lough

Australian Institute of Marine Science, Cape Ferguson, PMB3, Townsville, Queensland 4810, Australia

Abstract

We analyzed the contributions of clouds, turbidity, and tides to variations in irradiance and predicted benthic primary productivity on a coastal coral reef over a period of 2 yr (2001–2002). At 1.5 m below lowest astronomical tide (3.8-m tidal range), attenuation by suspended solids (turbidity) accounted for 74–79% of the total annual variation in irradiance, clouds for 14–17%, and tides for 7–10%. With increasing depth, the contribution from turbidity to irradiance variation increased asymptotically toward 95%. Fourier (spectral) analyses indicated that the benthic irradiance regime followed strong 8-week periodicities and weaker 2–4-week periodicities. The 8-week cycle was driven primarily by turbidity and secondarily by clouds and matches the periodicity of the intraseasonal Madden–Julian atmospheric oscillation. The weaker 3–4-week irradiance cycle was driven by turbidity; the 2-week cycle was driven by tides and, to a lesser extent, clouds. Comparisons of the benthic irradiance pattern with predictions of physiologically optimal irradiance levels (parameter E_k) for the coral *Turbinaria mesenterina* suggested that corals at the site alternate between states of potential light limitation and light stress, with a 2–8-week periodicity caused mainly by variations in turbidity. The effect of external sources of light reduction, such as episodic runoff events, on the energetics of benthic primary producers is likely to vary critically with the timing of such events.

Light is the primary resource for most of Earth's biological communities and provides the basis for the high productivity of tropical coral reefs (e.g., Barnes and Chalker 1990; Hatcher 1990). In aquatic environments, variations in the light field occur in both space and time, driven by patterns of cloud formation (Wright 1997) and concentrations of suspended or dissolved matter (e.g., *see* review by Kirk 1994). Variations in the light field above and below the water surface have implications for the temporal patterns of energy balance for aquatic primary producers over a range of time-scales, in particular for benthic, sessile organisms that are unable to modulate short-term changes in habitat irradiance. Although rigorous theoretical and conceptual frameworks exist for investigating adaptive responses of aquatic primary producers to variations in irradiance (Cullen and Lewis 1988; Prezelin 1992; Geider et al. 1996; *see also* review by Falkowski and Raven 1997; Anthony and Hoegh-Guldberg 2003), no studies have analyzed temporal variation in the benthic light field to quantitatively assess the relative contributions from cycles of meteorologic (e.g., clouds, wind), oceanographic (tides), and water quality (e.g., turbidity) factors to such irradiance variation.

At least four key factors affect temporal patterns of light variation in benthic habitats: (1) the seasonal pattern of daily surface irradiance (insolation), which is governed, in part, by the solar declination cycle (Kirk 1994); (2) variations in

clouds (Wright 1997; Mumby et al. 2001), which affect patterns of surface irradiance, particularly in wet, tropical regions; (3) transmittance through the water column, which depends on the optical properties of the water, most notably turbidity (van Duin 2001); and (4) tides, which can vary in range up to 14 m (Pond and Pickard 1983; Kleypas 1996) and which affect the depth of the water column and the amount of light transmitted to the benthic habitat. Variation in clouds can be considered a series of episodic events superimposed on a seasonal component (e.g., Wright 1997). Variation in turbidity is likely to follow a similar pattern because turbidity in many coastal environments is caused mainly by resuspension of bottom sediments through wave action (Larcombe et al. 1995) and thus episodic weather events. Conversely, tides follow a more systematic and predictable astronomic cycle (Allen 1997). Although such examples are intuitive, the combined effect of variations in clouds, turbidity, and tides on the weekly to monthly light variation is unknown for most coastal benthic habitats. Similarly, the individual relative contributions of these environmental factors to the temporal pattern of benthic irradiance have not been quantified, and the question remains as to how they interact. If light availability for benthic communities shows multiple periodicities, it will have consequences for temporal patterns of primary productivity, light stress, or both. Furthermore, in particular habitats in which light periodically becomes limiting for growth (e.g., in deep and turbid waters), the effect of external sources of light reduction on the health or stress status of benthic primary producers might depend critically on their timing relative to the natural irradiance pattern.

The purpose of this study was to examine the relative contributions of clouds, turbidity, and tides to the temporal variation in photosynthetic irradiance reaching subtidal reef benthos on a coastal, turbid-zone reef in the Great Barrier Reef lagoon (Queensland, Australia). Using predictions of subsurface irradiance over 2 yr, we analyze whether significant cyclical patterns of irradiance result from interactions between the above environmental factors. Furthermore, with a dynamic photosynthesis–irradiance model, which formally accounts for photoacclimation, we analyze the effect of the benthic irradiance pattern on temporal patterns of potential light limitation and light stress (photoinhibition) of primary producers with the use of photosymbiotic reef corals as a case study.

Methods

Study location—Cleveland Bay (Fig. 1) is a shallow, north-facing embayment of around 320 km^2 in area, relatively protected by Cape Cleveland from southeasterly trade winds that persist for the dry season of April–November and produce a regional northward longshore current and associated swell waves (e.g., Larcombe et al. 1995). Despite the regional dominance of the trade winds, Cleveland Bay is also influenced by northeasterly sea breezes that develop in the afternoon (e.g., Australian Bureau of Meteorology 1995). The wave climate within Cleveland Bay reflects the regional southeasterly-generated waves from the Great Barrier Reef
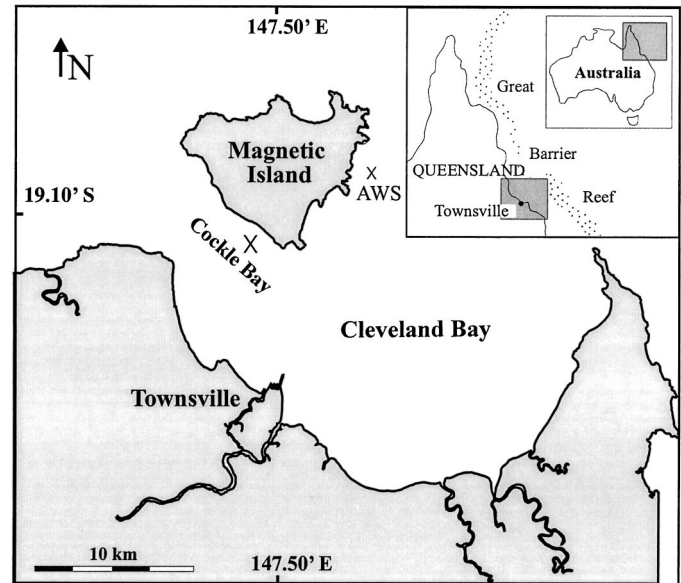

Fig. 1. Location of the study site, a turbid-zone fringing coral reef, in Cockle Bay (Townsville, north Queensland) and location of the Great Barrier Reef Marine Park Authority, Australian Institute of Marine Science weather station (AWS). At the study site, light loggers with automated sensor wipers were deployed on the sandy/muddy bottom immediately off the slope of the reef (~1.5 m below lowest astronomical tide).

continental shelf (Larcombe et al. 1995), which are refracted off Cape Cleveland into the bay with a mean period of 4.9 s and average significant wave height of 0.66 m (Department of Environment 1997). In Cleveland Bay, at depths of 5 m, resuspension of bottom sediment by waves occurs on an estimated 220 d yr^{-1} (Orpin et al. 1999), producing near-bed suspended sediment concentrations in excess of 20 mg L^{-1}. Tides are dominantly semidiurnal, with a strong diurnal inequality. A more complete overview of the oceanography of Cleveland Bay is summarized in Larcombe et al. (1995). We recorded benthic irradiances during 2–3-month periods on a west-facing reef slope in Cockle Bay (Magnetic Island) in the northwestern part of Cleveland Bay.

To determine the relative contributions of clouds, turbidity, and tides to the variation in light availability for reef benthos, we analyzed data on surface irradiance, benthic irradiance and associated light extinction, and tides for Cockle Bay for 2001 and 2002. All variables used in this paper are given in Table 1. Specifically, five data sets, model predictions, or a combination of both were used in the analyses: (1) observed surface irradiance (insolation), (2) estimated daily insolation maxima (cloudless skies), (3) light attenuation through the water column during three 2–3-month periods, (4) observed tidal changes, and (5) predicted long-term light attenuation patterns estimated from measured local wind speed and direction. As a basis for determining the relative contribution of each factor (clouds, turbidity, tides) to the pattern of irradiance variation near the benthos, irradiance patterns were compared under four environmental scenarios: (A) cloudless skies, (B) cloud variation, (C) turbidity and cloud variation, and (D) cloud, turbidity, and tidal

Table 1. Notation.

Symbol	Interpretation	Unit
b	Exponent relating irradiance attenuation to wind speed	Dimensionless
$\bar{E}_S$	Observed surface irradiance, averaged over the day	μmol quanta m^{-2} s^{-1}
$\bar{E}_S'$	Surface irradiance under cloudless skies, averaged over the day	μmol quanta m^{-2} s^{-1}
$E_0(t)$	Irradiance immediately below the surface as a function of time of day, corrected for reflectance	μmol quanta m^{-2} s^{-1}
$\bar{E}_0$	Irradiance immediately below the surface averaged over the day, corrected for reflectance	μmol quanta m^{-2} s^{-1}
$E(z, t)$	Irradiance as a function of depth and time of day	μmol quanta m^{-2} s^{-1}
$\bar{E}(\bar{k}_D, \bar{z})$	Irradiance as a function of the attenuation coefficient and depth, averaged over the day	μmol quanta m^{-2} s^{-1}
E_k	Subsaturation irradiance of the photosynthesis–irradiance curve	μmol quanta m^{-2} s^{-1}
E_{kS}	Subsaturation irradiance at steady state	μmol quanta m^{-2} s^{-1}
E_{kMS}	Maximum subsaturation irradiance	μmol quanta m^{-2} s^{-1}
h	Tidal height above lowest astronomical tide	m
$\bar{k}_D$	Irradiance (PAR) attenuation coefficient (daily average)	m^{-1}
k	Coefficient relating wind speed to $\bar{k}_D$	m^{-1}
P_{max}	Maximum rate of photosynthesis, averaged over the day	μmol O$_2$ cm^{-2} h^{-1}
t	Time	hours
T	Time	days
$\bar{U}$	Wind speed, averaged over 24 h	m s^{-1}
$\bar{U}_m$	Maximum observed wind speed (daily average)	m s^{-1}
$z(t)$	Depth as a function of time of day	m
$\bar{z}$	Depth, averaged over 24 h	m
ζ	Coefficient for the kinetics of photoacclimation	Dimensionless

height variation (*see summary in Table 2*). The variance contribution from individual factors was then obtained from the difference in daily irradiances between two scenarios. We construct these scenarios in the following sections.

Effects of clouds: Observed versus maximum surface irradiance—Data on half-hourly surface irradiance (E_S) for Cleveland Bay were obtained from the joint Great Barrier Reef Marine Park Authority–Australian Institute of Marine Science weather station (19°9′S, 146°53′E) located ~10 km from Cockle Bay (Fig. 1) and converted to daily average irradiances ($\bar{E}_S$). Because we used daily averages, hourly variation in clouds between the field site and the weather station was averaged during the day. Surface irradiance data for periodic deployments of surface loggers at the field site were consistent with those of the weather station (<5% variation in daily irradiances). To determine the relative light extinction by clouds and its temporal pattern, we compared $\bar{E}_S$ (scenario B, Table 2) with insolation expected in the absence of clouds ($\bar{E}_S'$, scenario A). Models for predicting maximum insolation at a given geographic location are presented in Kirk (1994). For simplicity, we estimated $\bar{E}_S'$ empirically by determining insolation maxima within 2-week windows (i.e., rolling maxima). The effect of clouds on surface irradiance as a function of time was then estimated as the difference between the insolation maximum during the 2-week window and observed insolation at a given day ($\bar{E}_S' - \bar{E}_S$; *see Table 2*). The method is appropriate in areas where clouds are absent most of the time and might, in this study, underestimate maximum insolation only slightly.

Effects of turbidity—Irradiance (daily average) as a function of turbidity and water depth was estimated with Lambert–Beer's law

$$\bar{E}(\bar{k}_D, \bar{z}) = \bar{E}_0 \exp(-\bar{k}_D \bar{z}) \tag{1}$$

where $\bar{E}_0$ is the average irradiance immediately below the surface on a given day, $\bar{z}$ is the average water depth (m), and $\bar{k}_D$ is the average extinction coefficient for irradiance within the photosynthetically active range (PAR, 400–700 nm). Suspended sediment is the major contributor to light attenuation in Cleveland Bay (Ridd unpubl. data), which justifies the use of a unique irradiance attenuation coefficient (van Duin 2001). The relative role of seasonal phytoplankton variability in light extinction was assumed to be of minor

Table 2. Summary of model scenarios used to estimate the effects of clouds, turbidity, and tides on the temporal variation in irradiance for the benthos at a fringing coral reef (Cockle Bay, north Queensland, Australia). The depth below lowest astronomical tide was 1.5 m, and the tidal range for the adjacent Magnetic Island (Townsville) is 3.8 m. See Table 1 for parameters.

		Parameter		
Source of variation	Scenario	Surface irradiance	Irradiance attenuation ($\bar{k}_D$)	Depth ($\bar{z}$)
Clear skies	A	2-week rolling Maxima, $\bar{E}_S'$	Constant (Annual mean=0.385 m^{-1})	Constant (Annual mean=3.4 m)
Clouds	B	Observed, $\bar{E}_0$	Constant (0.385 m^{-1})	Constant (3.4 m)
Clouds+turbidity	C	Observed, $\bar{E}_0$	Variable, $\bar{k}_D$	Constant (3.4 m)
Clouds+turbidity+tides	D	Observed, $\bar{E}_0$	Variable, $\bar{k}_D$	Variable ($\bar{z}$=1.5 m+tidal height)

importance because chlorophyll concentrations rarely exceed 4 μg L^{-1} in the Great Barrier Reef lagoon (Brodie et al. 1997). Although the specific irradiance extinction coefficient of chlorophyll is higher than that of inorganic particles (van Duin 2001), concentrations of suspended sediment in Cleveland Bay are several orders of magnitude higher than chlorophyll concentrations at all times (Muslim and Jones 2003). We estimated $\bar{E}_0$ from $\bar{E}_S$ after adjustment for surface reflectance (R), which was estimated from data by Austin (1974; for details, *see Web Appendix 1,* http://www.aslo.org/lo/toc/vol_49/issue_6/2201a1.pdf). Transmittance through the surface was thus calculated as 100% − R, and $\bar{E}_0$ was estimated as $E_S(t)$(100% − R). The accuracy of surface transmittance estimates was of secondary importance because our primary focus was to study temporal patterns of benthic irradiance variation rather than to determine absolute benthic irradiance.

Long-term estimates of $\bar{E}(\bar{k}_D, \bar{z})$ were obtained by a three-step approach. First, benthic (downwelling) irradiance was recorded continuously (half-hourly) during three periods of 2–3 months during the 2 yr (2001–2002). Second, patterns of light attenuation were estimated for the entire period by a predictive model of $\bar{k}_D$ as a function of local wind data, calibrated against the three periods of observed $\bar{k}_D$. On inshore fringing reefs along the Queensland coast, the variation in turbidity is primarily governed by regional wave-driven resuspension, augmented to some extent by tides and currents (Larcombe et al. 1995; Orpin et al. 1999). Third, subsurface irradiance as a function of $\bar{k}_D$ and depth was predicted for the 2-yr period by Eq. 1 and the parameter values obtained in step 2.

Empirical $\bar{k}_D$ data for Cockle Bay were obtained as light extinctions through the water column, measured by automated data loggers (Model 392, DataFlow Systems) at the water surface and on the seabed (1.5 m below lowest astronomical tide, LAT). The light sensors were cosine corrected, measuring within the 400–700-nm wave band (PAR), and calibrated against a manufacturer-calibrated Li 192S sensor (Licor) above or below water. The sensor on the seabed was equipped with an automated sensor wiper (Ridd and Larcombe 1994) to prevent biofouling. Tidal predictions for Townsville were obtained from the National Tidal Facility (Flinders University) and used to calculate the distance from the surface to the bottom sensor as a function of time of day. To maximize the accuracy of $\bar{k}_D$ estimates obtained by transmittance of natural sunlight, we used irradiance data within the 2-h window around noon, during which irradiance is maximized and reflectance is minimized (<5%; Kirk 1994). By rearrangement of Eq. 1 and by parameterization of variables by time of day (t), $\bar{k}_D$ was estimated as in Eq. 2.

$$k_D(t) = \ln[E_0(t)/E(z, t)]/z(t), \quad \text{for } 1000 \text{ h} < t < 1400 \text{ h} \quad (2)$$

For the purpose of analyzing day-to-day variations in irradiance attenuation, we assumed that midday $k_D(t)$ values approximated daily averages (i.e., $k_D(t) \approx \bar{k}_D$. To test whether estimates of $\bar{k}_D$ obtained from two-point irradiance measurements could be used to predict irradiances at intermediate depths with adequate precision, we measured the vertical profile of downwelling irradiance (PAR) using an array of five light loggers suspended between the surface ($\sim$0 m) and

the seabed at the foot of the reef slope ($\sim$5 m below LAT). Vertical irradiance profiles were recorded on four separate sampling occasions (continuous logging during 4-h periods around noon) to represent varying turbidity regimes.

Long-term predictions of $\bar{k}_D$ (and by inference, concentrations of suspended particles) in Cockle Bay were modeled as a function of wind speeds obtained from the nearby weather station in Cleveland Bay (Fig. 1). Resuspension of bottom sediments is a power function of current speed and wave height (Wright 1995), which in turn are functions of wind speed. To account for the lag time between the onset of a wind event and the buildup of waves, as well as the residence time of particles in the water column following resuspension, we constructed our model as a power series. The daily average attenuation coefficient ($\bar{k}_D$) of a given day (T) was thus modeled as

$$\bar{k}_D(\bar{U}, T) = k_0\left[\frac{\bar{U}(T)}{U_m}\right]^b + k_1\left[\frac{\bar{U}(T-1)}{U_m}\right]^b + \cdots$$
$$+ k_n\left[\frac{\bar{U}(T-n)}{U_m}\right]^b + \bar{k}_{D-\text{base}} \quad (3)$$

where $\bar{U}$ is the wind speed averaged over the previous 24 h; U_m is the maximum observed wind speed (set to 20 m s^{-1}), which was used to nondimensionalize the wind effect; T is time (days); k_0, k_1, and k_n are coefficients (m^{-1}) that determine the influence of present and past wind speeds on the present $\bar{k}_D$ level; b is an exponent; and $\bar{k}_{D-\text{base}}$ is the baseline attenuation. Preliminary analyses indicated that adjustment for wind direction did not increase the precision of the model for Cockle Bay. However, wind direction does affect wave regime (and thereby turbidity regime) differently between locations, depending on local geomorphology, bathymetry, and hydrodynamics (e.g., *see* Allen 1997). Also, tidal flows have only a minor influence on resuspension in the study area (Larcombe et al. 1995) and were not formally included in the model. To rigorously examine the precision and robustness of the model, Eq. 3 was first calibrated against the observed k_D values of the first two data blocks ($n = 251$ d) and then evaluated with the third data block ($n = 63$ d). The calibration was conducted with the use of iterative, nonlinear estimation (Statistica 2001, ver. 6.1, StatSoft Inc.), which produced value estimates and standard errors for each parameter. To evaluate the model, we used the parameter estimates for the calibration to produce predicted values for the third data block and then compared the distributions, means, and variances of $\bar{k}_D$ residuals from the evaluation against those from the calibration. Daily benthic irradiance averages as a function of depth ($\bar{z}$) and $\bar{k}_D$ for a given day were then obtained by Eq. 1. Confidence ranges for benthic irradiances were estimated by Monte Carlo analyses in which the parameters of Eq. 3 were sampled randomly (1,000 replicate runs) from within their normal distributions ($\pm$1 SD of the parameter estimate obtained with the use of the $\bar{k}_D$ model calibration).

To estimate the effect of turbidity variation on the temporal pattern of irradiance for the reef benthos in Cockle Bay, we compared two scenarios: (C) predicted irradiances at 3.4 m depth under variable turbidity and (B) predicted

irradiances at 3.4 m depth at constant $\bar{k}_D$ (annual average of 0.385 m^{-1}). The time series of differences (residuals) between these two scenarios provided a basis for estimating effects of turbidity on the temporal variation in irradiance (Table 2).

Effects of tides—Lunar days are ~50 min longer than solar days (e.g., Wright 1995) so that the effect of tides on the daily influx of light in the benthic habitat gradually intensifies and weakens over cycles of ~2 weeks. Superimposed on these short-term periodicities in light regime are spring–neap tidal cycles. Moreover, on a longer timescale, the variation in heights of spring and neap tides is governed by the vernal and autumnal equinoxes (Allen 1997). The maximum tidal range for Magnetic Island is 3.8 m, which is intermediate for locations along the Queensland coast. To determine the contribution of tidal regime to the variation in irradiance at 1.5 m below LAT plus tidal variation, we used the tidal predictions for years 2001 and 2002 for Townsville (National Tidal Facility, Flinders University) as an input variable into Eq. 1. The time series of differences (residuals) between irradiance predictions at constant depth (annual average of 3.4 m) and variable depth (1.5 m + variation in tides) was used to analyze the effect of tides on irradiance variation (scenarios C and D in Table 2).

Data analysis—The generated irradiance predictions were analyzed in three different ways. First, the relative contribution from each factor (clouds, turbidity, and tides) to the temporal variation in benthic irradiance over the year was determined as the mean squares (variances) of the differences (residuals) between each pairwise comparison of the four scenarios (i.e., A–B, B–C, and C–D in Table 2) divided by the mean squares of the total residuals (scenarios A–D, *see Table 2*). Mean squares (MS) of the residuals for the comparison of scenario A versus B, for example, were calculated as $\Sigma(A_i - B_i)^2/n$, where i denotes time (day) and n is the total number of days. Thus, the variance contribution from clouds (V_{Clouds}), turbidity ($V_{Turbidity}$), and tides (V_{Tides}) were

$$V_{Clouds} = MS_{ResAB}/MS_{ResAD} \qquad (4.1)$$

$$V_{Turbidity} = MS_{ResBC}/MS_{ResAD} \qquad (4.2)$$

$$V_{Tides} = MS_{ResCD}/MS_{ResAD} \qquad (4.3)$$

where the sum of the three variance components equals 1. Confidence ranges for the variance contributions were estimated by Monte Carlo analyses (*see Methods: Effects of Turbidity*). Second, to evaluate the role of each factor in the periodicity of the benthic irradiance pattern, the time series of irradiance differences (residuals) between scenarios A versus B, B versus C, and C versus D were all subjected to Fourier (spectral) analyses (*see* Bloomfield 1976; Priestley 1981; Shumway 1988) with the use of the time series module in Statistica (ver. 6.1). This provided a means of assessing the relative strength of periodicities, indicated by spectral densities in the data. Because the irradiance data set was limited to a 2-yr period, the results of Fourier analyses focused on intraseasonal periodicities only.

Third, to compare the predicted temporal pattern in irra-

diance with the physiologically optimal irradiance of a selected group of benthic photosynthetic organisms in Cockle Bay, we estimated the variation in the dynamic subsaturation parameter (E_k) of the photosynthesis–irradiance response curve of the scleractinian coral *Turbinaria mesenterina.* The dynamic model describing the relationship between E_k and irradiance variation in this species has been described and tested previously (Anthony and Hoegh-Guldberg 2003). E_k can be expressed formally as

$$E_k(\bar{E}, T) = E_{kS}(\bar{E}) + \zeta[E_{kS}(\bar{E}) - E_k(T - 1)] \qquad (5)$$

where ($\bar{E}$) is daily average irradiance, T is time (days), and ζ is a dimensionless coefficient characterizing the daily rate of change in E_k (*see Web Appendix 1*) toward the predicted steady-state value given by Eq. 6.

$$E_{kS}(T) = E_{kMS}\left[\frac{\bar{E}(\bar{k}_D, \bar{z}, T)}{\bar{E}_{max}}\right]^{\beta_2} \qquad (6)$$

E_{kMS} is the maximum value obtained under maximum average irradiances ($\bar{E}_{max} \approx 800$ μmol quanta m^{-2} s^{-1}) and β_2 is an exponent. For *T. mesenterina,* $\zeta \approx 0.86$ (*see Web Appendix 1*), which is high for benthic primary producers (Anthony and Hoegh-Guldberg 2003) and thus provides a conservative basis for analyzing to what extent current irradiance is suboptimal or supraoptimal. Daily average irradiances lower than the current E_k potentially indicate light limitation, whereas irradiances higher than E_k could lead to photoinhibition.

Rates of gross photosynthesis (P_g) parameterized by daily average irradiance and time (days) were predicted as

$$P_g(\bar{E}, T) = \left[P_{max}(T)\tanh\frac{\bar{E}(T)}{E_k(T)}\right] \qquad (7)$$

where $P_{max}(T)$ is the dynamic maximum rate of gross photosynthesis (*see Web Appendix 1*). To examine periodicities in rates of coral photosynthesis, the 2-yr predictions of Eq. 6 were subjected to Fourier (spectral) analysis (*see Methods: Data Analysis*).

Results

Effects of clouds on surface irradiance—The pattern of observed surface irradiances in Cleveland Bay showed large deviations from the 2-week rolling maxima, indicating strong variation in irradiance attributable to clouds (Fig. 2). Episodically, observed insolation during summer was less than 20–40% of the rolling maxima, and for most of February 2001 (days 32–59), surface irradiances were <70% of the rolling maxima. The large drops in irradiance during the second half of February 2001 coincided with the passage of tropical cyclones Wylva and Abigail in the north Queensland area (www.bom.gov.au). The week-long 50–80% drop in surface irradiance during February 2002 was a result of widespread thunderstorms associated with an active monsoon trough. The observed patterns in insolation can almost certainly be attributed to variation in clouds and not to incidental fouling of the sensors because data patterns were consistent between the weather stations in Cleveland Bay and Cape Bowling Green Bay (located ~50 km apart).
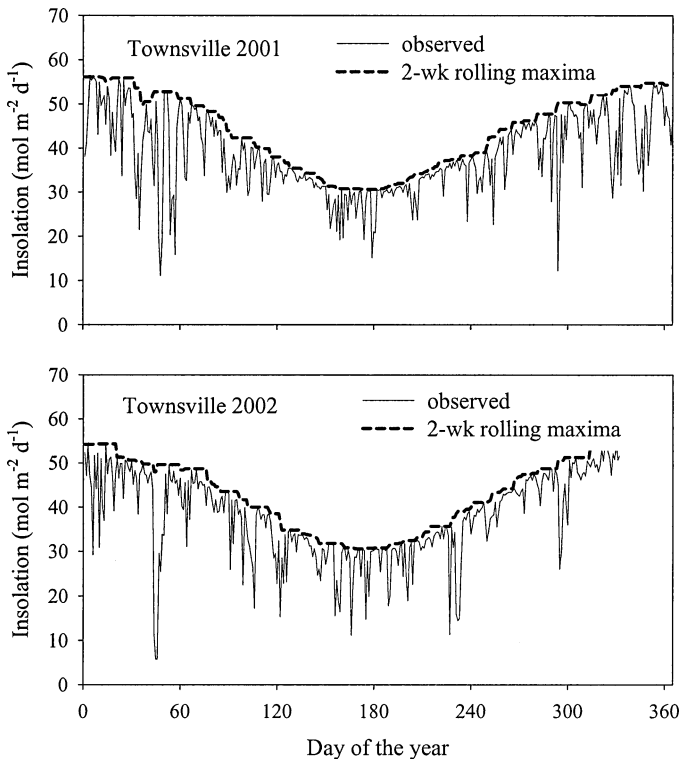
Fig. 2. Daily surface irradiance (insolation) for Townsville (north Queensland, Australia) during 2001 and 2002. Two-week rolling maxima were used to approximate surface irradiances under a cloudless sky. Residuals between observed irradiances and the rolling maxima were used to analyze temporal variations in clouds.

Effects of turbidity on patterns of benthic irradiance—
Nonlinear regressions of the repeated vertical irradiance distributions indicated that the irradiance attenuation coefficient of the Lambert–Beer equation ($\bar{k}_D$) was estimated with high precision (Fig. 3). Specifically, the model explained between 95% and 99% of the variation, and standard errors of $\bar{k}_D$ were <5% of the parameter estimates.

Irradiance attenuation, and hence benthic irradiance, could be predicted relatively precisely from local wind data (Fig. 4). Specifically, Eq. 3 explained 70% of the variation in $\bar{k}_D$ of the first two data blocks (Table 3). Variation in $\bar{k}_D$ was best explained with the use of three wind speed coefficients (k_0, k_1, and k_2), beyond which additional coefficients became nonsignificant. A Kolmogorov–Smirnov test indicated that the residuals were normally distributed ($p > 0.20$), and their behavior indicated minimal structural bias of the model (Fig. 5A). Importantly, the behavior of the residuals for the model evaluation (Fig. 5B, with predicted $\bar{k}_D$ values based on the parameter estimates of the calibration) corresponded closely to those of the calibration. Specifically, a *t*-test followed by a Levene's test showed that the means and variances of the residuals did not differ significantly between the calibration and the evaluation ($p = 0.337$ and $p = 0.201$, respectively). These results demonstrate that the model is robust and capable of forecasting with acceptable precision.

Daily average irradiances at 1.5 m below LAT (mean water depth, 3.4 m), as predicted from patterns of surface ir-
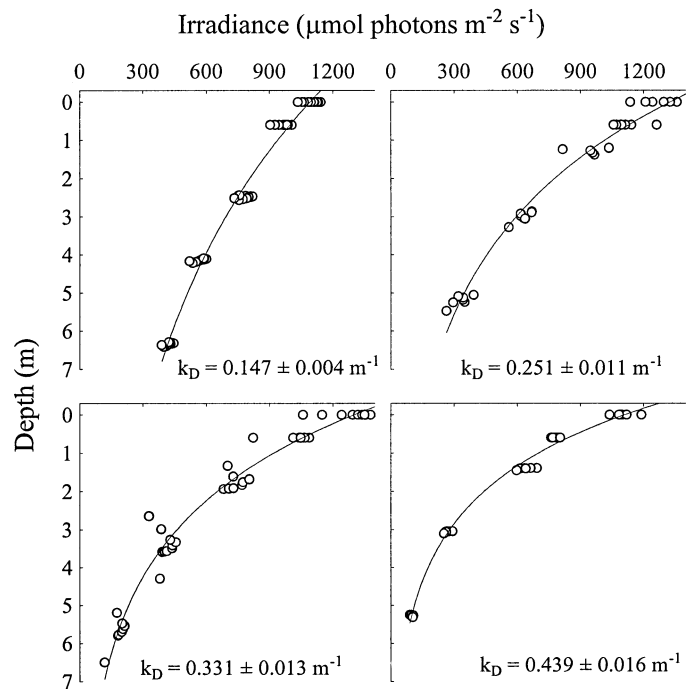

Fig. 3. Vertical profiles of downwelling irradiance near a coral reef in Cleveland Bay at four sampling occasions in June/July 2000. Equation 1 (Lambert–Beer's law) provided a good fit to the data for all occasions (97–99% explained variation), and the light attenuation coefficient was estimated with high precision (SE < 5% of parameter estimates).

radiance ($\bar{E}_s$), attenuation ($\bar{k}_D$), and tides ($\bar{E}[\bar{k}_D, \bar{z}]$), varied by more than an order of magnitude and were less than 50–100 μmol quanta m^{-2} s^{-1} for periods of up to 2 weeks (Fig. 6). For most days, irradiances incident on the benthos were
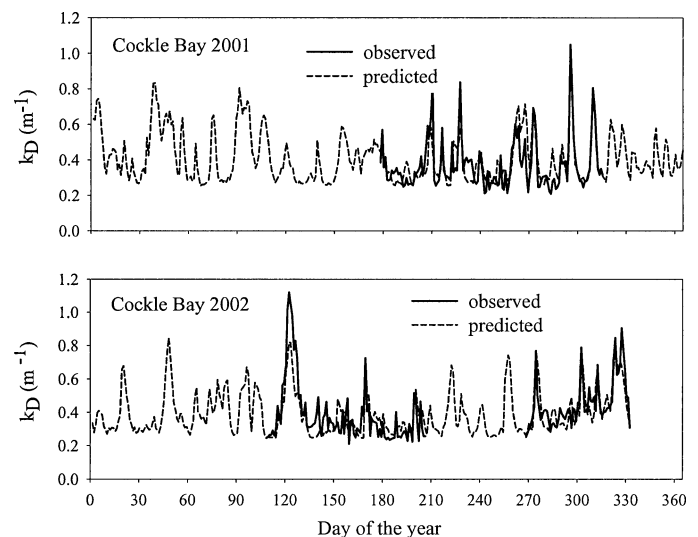

Fig. 4. Observed versus predicted benthic irradiances during 2001 and 2002. The pattern in benthic irradiance was estimated (dashed line) from local wind data with Eq. 3, which was calibrated against the two first periods of observed irradiances (solid line). The model explained ~70% of the variation (*see also Table 3*).

Table 3. Results of nonlinear regressions for observed (estimated) irradiance attenuation ($\bar{k}_D$) in Cockle Bay versus wind speeds at a nearby weather station (*see Fig. 1*) with the first two of three data blocks ($n = 284$ d) in years 2001 and 2002. Benthic irradiance was measured at 1.5 m below lowest astronomical tide (LAT). Predicted and estimated irradiance attenuations ($\bar{k}_D$) are shown in Fig. 3.

Parameter	Estimate	SE	p	R^2
k_0	0.837	0.056	<0.001	0.70
k_1	0.234	0.065	<0.001	
k_2	0.158	0.049	0.001	
b	4.200	0.438	<0.001	
k_{D-base}	0.267	0.007	<0.001	

Fig. 5. Predicted versus observed attenuation coefficients ($\bar{k}_D$) for the (A) model calibration using the first two data blocks ($n = 251$ d), and (B) model evaluation with predictions based on the calibration and observed data from the third data block ($n = 63$ d). In both cases, the residuals were normally distributed around the unity line, and the means and variances did not differ significantly between calibration and evaluation (*see text* for details).

<30% of surface irradiances. The calculated standard deviations around the predicted benthic irradiances (by Monte Carlo analysis) were less than ~14% of the estimates, further indicating a relatively high precision of $\bar{k}_D$ model predictions.

Variance contributions from clouds, turbidity, and tides— Fluctuations in average daily irradiance resulting from turbidity were more than three times stronger than fluctuations resulting from clouds and 10 times those from tidal changes (Fig. 7). Specifically, the partitioning of mean squares of the residuals for the three scenario comparisons indicated that turbidity, clouds, and tides accounted for around 76%, 15%, and 8% of the total predicted irradiance variation, respectively (Table 4). On the basis of Monte Carlo confidence ranges (Table 4), imprecision of the $\bar{k}_D$ wind model parameters caused only around 3–13% uncertainty in the irradiance variance contributions for each factor. Separate comparative analyses of irradiance variance contributions with the observed and predicted $\bar{k}_D$ values for the three data blocks only (*see Fig. 4*) further demonstrated concordance between model (Eq. 3) and data. Specifically, for these time windows, the variance contributions from turbidity (86.9%), clouds (7.5%), and tides (5.6%) estimated with observed $\bar{k}_D$ values were well within the confidence range of the variance contributions estimated with predicted $\bar{k}_D$ values: 80.1–89.0%, 6.3–11.1%, and 4.9–8.8%, respectively.

To investigate the effect of depth on the relative variance contribution from each factor, we generated additional simulations of irradiance for depths of 0–5 m below LAT. These analyses assumed that turbidities near the benthos at the reef flat and crest (near LAT) and at the foot of the reef slope (~5 m below LAT) are similar to measured turbidities at 1.5 m depth below LAT. However, given equivalent sediment availability, sediment resuspension by a given wave energy is greater in shallow compared with deeper water (e.g., Wright 1995; Allen 1997), and these predictions are likely to underestimate the effect of turbidity on light extinction in shallow water and vice versa in deeper water. Near LAT, the average predicted contribution from clouds, turbidity, and tides to the variation in irradiance was around 30%, 55%, and 15%, respectively (Fig. 8). At 5 m below LAT, clouds and tides each contributed only around 3–4% to the irradiance variation so that with increasing depth, the variance
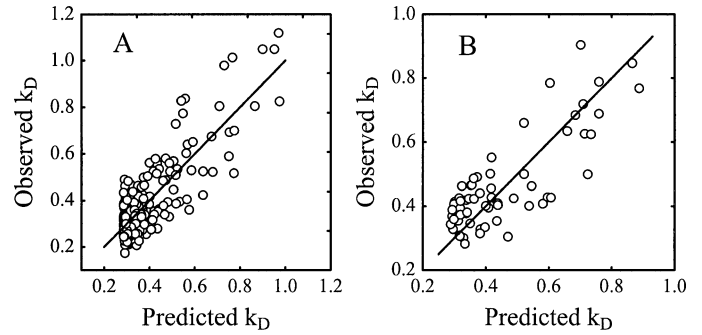
contribution from turbidity increased asymptotically toward ~95%.

Irradiance periodicities— The periodic density pattern of irradiance residuals for clouds and turbidity separately (scenarios A–B and B–C, respectively) and for clouds, turbidity, and tides in combination (scenario A–D) indicated that the periodicities of clouds and turbidity were largely synchronous around the 8-week period but tended to be asynchro-
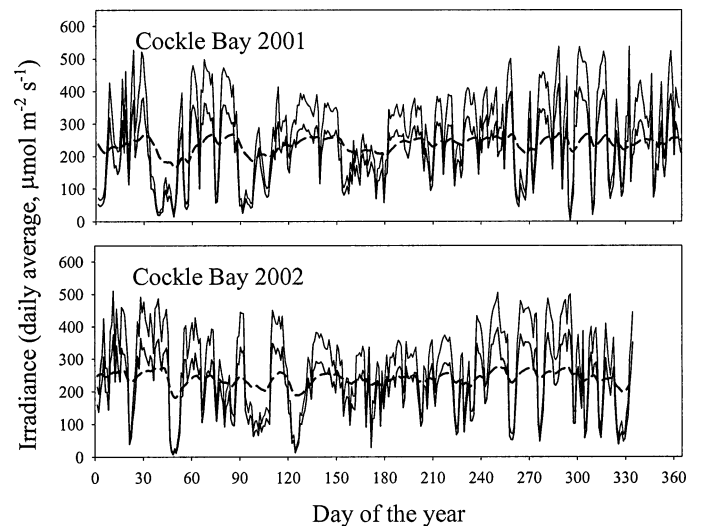

Fig. 6. Predicted benthic irradiance at 1.5 m below lowest astronomical tide (LAT) in Cockle Bay during 2001 and 2002. Data are upper and lower confidence limits (mean ± 1 SD) of the average irradiance during the day ($\bar{E}(\bar{k}_D, \bar{z})$) estimated with Eqs. 1 and 3. Confidence limits were estimated with the use of multivariate Monte Carlo analyses (*see text*). The dashed line indicates the predicted subsaturation constant (E_k) for the photosynthesis–irradiance response of the coral *Turbinaria mesenterina* with a 15% per day rate of photoacclimation (Anthony and Hoegh-Guldberg 2003; *see also Web Appendix 1*). Irradiances $<E_k$ are suboptimal and indicate light-limited growth, and irradiances $>E_k$ are supraoptimal, potentially leading to photoinhibition.
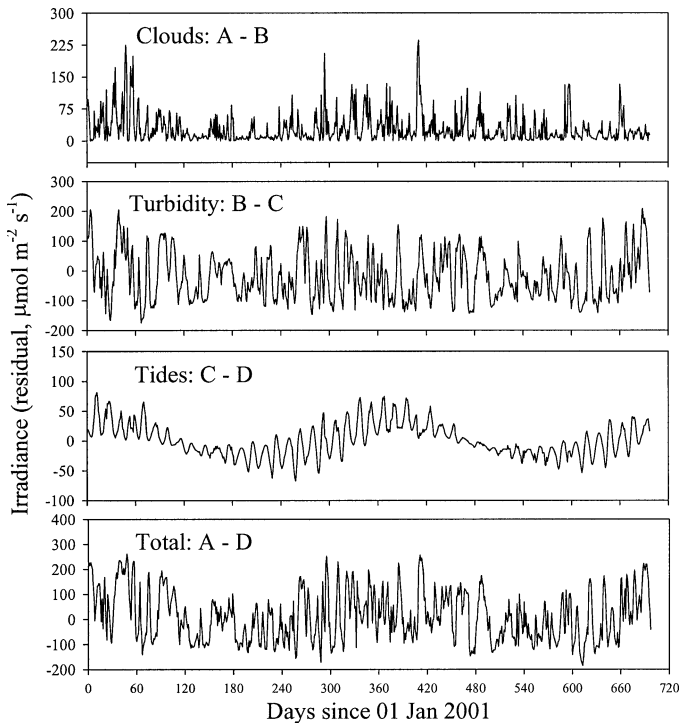
Fig. 7. Irradiance residuals for comparison of the four scenarios outlined in Table 2 during 2001 and 2002 combined. The temporal variation and amplitude of residuals for clouds, turbidity, and tides are indicative of their variance contributions to the overall variation in irradiance near the benthos. Note different scales on the *y*-axes.

nous at shorter (3–4-week) periodicities (Fig. 9). Fourier analysis of residuals for the effects of tides (scenarios C–D) produced distinct 2-week periodicities, as predicted from the difference in solar and lunar periodicities. However, because the amplitude of the residuals for turbidity was several times greater than those of clouds and tides, the overall pattern of irradiance residuals (scenarios A–D) was largely governed by variation in turbidity. Repeated Fourier analyses of the irradiance residuals after random rearrangement of the time series indicated that spectral densities at periods of 2, 3–4, and 8 weeks in the total irradiance pattern were significantly higher than maximum spectral densities expected from a random (white noise) time series (Fig. 9, dashed lines).

Temporal patterns in predicted productivity—Estimated irradiances at 1.5 m below LAT in Cockle Bay fluctuated strongly around the predicted subsaturation irradiances (E_k) of the coral species *T. mesenterina* (Fig. 6), indicating alternating periods of potential light limitation ($\bar{E}(\bar{k}_D, \bar{z}) \ll E_k$) and photoinhibition ($\bar{E}(\bar{k}_D, \bar{z}) \gg E_k$). The parameter E_k in the dynamic photosynthesis–irradiance model is a key indicator of the state of photoacclimation (Anthony and Hoegh-Guldberg 2003) and provides a proxy for the optimal irradiance at a given point in time. During periods of thick cloud cover, high turbidity, or both, particularly in February and March/April 2001 and February and May 2002, irradiances fell episodically to below a third of E_k (Fig. 6). Conversely, during periods of clear skies and low turbidity, irradiances were almost twice the predicted E_k level. Over the year, E_k varied

Table 4. Results of residual analyses for the comparison of the scenarios of clouds, turbidity, and tidal regime outlined in Table 2. The analyses were based on the irradiance predictions (Eqs. 1, 3) for the full 2-yr period. Variance contributions from each factor were calculated with Eq. 4. Confidence ranges ($\pm 95\%$) were determined by Monte Carlo analysis and pertain specifically to the estimation error of the diffuse attenuation coefficient ($\bar{k}_D$, *see text for details*).

Factor	Scenario comparison	Variance contribution (%)	Confidence range (%)
Clouds	A–B	15.2	13.5–17.2
Turbidity	B–C	76.4	73.7–78.9
Tides	C–D	8.4	7.4–9.6
Total	A–D	100	N/A

by <25% because it was constrained by the kinetics of photoacclimation (Anthony and Hoegh-Guldberg 2003; *see Web Appendix 1*).

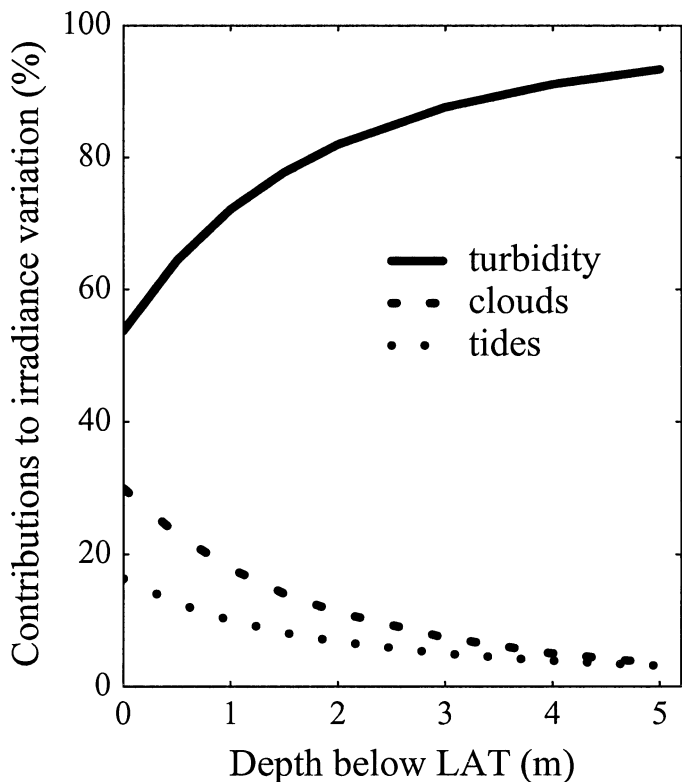Analyses of the 2-yr predictions of daily gross photosyn-

Fig. 8. Changes in estimated relative contributions from clouds, turbidity, and tides to the variation in benthic irradiance with increasing depth below lowest astronomical tide (LAT). Average irradiance during the day ($\bar{E}(\bar{k}_D, \bar{z})$) as a function of irradiance attenuation ($\bar{k}_D$) and depth ($\bar{z}$) was predicted with Eq. 1, and variance contributions were calculated with Eq. 4. The prediction does not account for the enhanced effect of tides and resuspension in shallow water and assumes similar distributions of particles in water columns of varying height (depth). In clear-water habitats, the minimum variance contribution from turbidity is likely to be negligible compared with the prediction here for a turbid-zone reef (~55%).

Fig. 10. Fourier (spectral) analysis of predicted rates of gross photosynthesis (daily average) of a coral species (*Turbinaria mesenterina*) with the predicted irradiance data in Fig. 6 as the input variable. Rates of photosynthesis were adjusted for photoacclimation by the model of Anthony and Hoegh-Guldberg (2003).
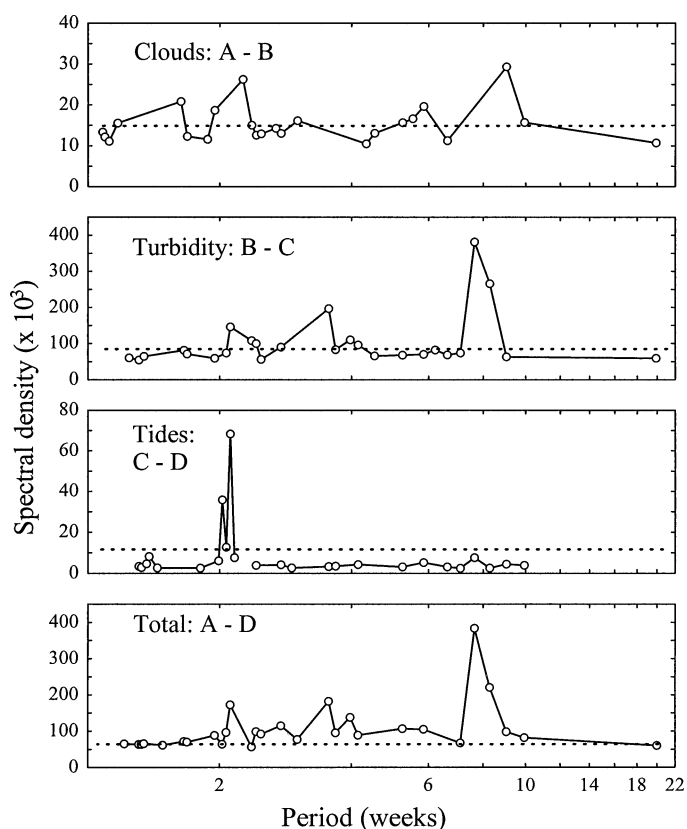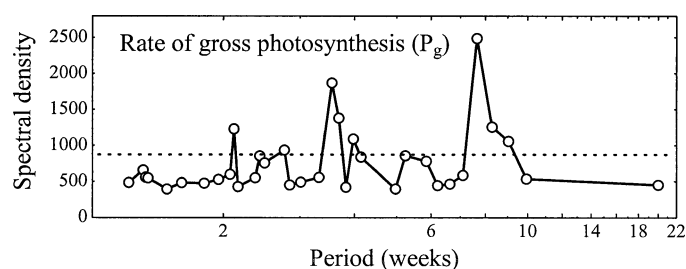
Fig. 9. Fourier (spectral) analyses of irradiance residuals for the four comparison scenarios in Fig. 7. Spectral density is a measure of the number of adjacent frequency regions that contribute to the overall periodic behavior of the time series. The plots were generated with the use of the 30 highest spectral densities only. The dashed line indicates the maximum spectral density (confidence limit) determined from Fourier analyses of the time series after repeated, random reorganizations of the data (white noise). Note different scales on the *y*-axes.

thesis for *T. mesenterina* at 1.5 m below LAT showed strong 8-week periodicities (Fig. 10), consistent with analysis of the irradiance residuals (scenario A–D). However, the strengths of the 3–4-week and 2-week periodicities in gross photosynthesis were relatively higher than in the irradiance data set. In particular, the strength of the 3–4-week periodicity was more than 65% of the 8-week periodicity. The relatively greater strengths of short periodicities in the photosynthesis data are mainly due to a reduction in photosynthesis variation over longer (e.g., 2-month) timescales as a result of photoacclimation (i.e., an absolute decrease in the strength of long periodicities).

Discussion

With the use of an inshore turbid-zone reef as a case study, our results demonstrate that daily irradiances at the seabed in coastal marine habitats can frequently fall to <10% of irradiance maxima for periods of 1–2 weeks. Benthic irradiances varied dramatically during the 2-yr study period and demonstrated strong 8-week and weaker 3–4-week period-

icities, driven primarily by variations in irradiance attenuation by the water column (i.e., turbidity) and secondarily by changes in clouds. Tides produced a distinct 2-week irradiance periodicity, as predicted from the mismatch between solar and lunar cycles, and contributed significantly to the overall irradiance pattern. Previous studies of benthic irradiance have been at a range of timescales (e.g., Dunton 1994), but our work is the first to analyze intraseasonal cyclic patterns to quantify the relative contributions of the main environmental factors to the temporal variation in irradiance and to predict the associated patterns in benthic primary productivity.

The measured benthic irradiance field at the inshore, turbid-zone reef is characterized by high temporal variation on a timescale of days to a year. Variation in the irradiance attenuation coefficient because of turbidity contributed nearly 80% to the overall irradiance variation. Analyses of the variance components of the benthic irradiance pattern, however, indicate that the relative importance of clouds, turbidity, and tides depends strongly on the depth below LAT (Fig. 8). By extending these analyses to other turbidity and tidal regimes, two generalizations emerge. First, given a similar cloud pattern, the variation in irradiance in shallow, clear-water habitats (e.g., oceanic reefs) will be driven mainly by clouds and will thus display considerably less irradiance variation compared with that of coastal habitats at a similar depth. In such cases, the variance contribution from turbidity to the benthic irradiance pattern will be significant in deep water only. Second, in areas with maximum tidal ranges greater than those of our study site (Townsville, ~3.8 m), the variance contribution from tides will be more significant and will covary with the variance contribution from turbidity, primarily because the irradiance attenuation coefficient ($\bar{k}_D$) and water depth ($\bar{z}$) form a product in Lambert–Beer's law (Eq. 1). The cyclical pattern in benthic irradiance driven by tides is consistent with the temporal productivity pattern observed for marine intertidal microphytobenthos (Serodio and Catarino 2000). Furthermore, tidal currents, and thereby the resuspension of solids in shallow water, tended to increase in magnitude with tidal range (Wright 1995; Allen 1997), thus strengthening the fortnightly irradiance cycle—particularly in shallow water. On the basis of the results of previous studies in the area (Larcombe et al. 1995), however, we concluded that resuspension by waves is the key mech-

anism driving turbidity patterns in Cleveland Bay and that tidal currents play a minor role. This is substantiated by the strong fit of the predicted irradiance attenuations to measured wind speeds (Fig. 4; Table 3) and the associated model evaluation (Fig. 5). The analysis of variance contributions from turbidity can be extended to include irradiance patterns in some lakes because mechanisms of resuspension are largely similar to those in coastal marine habitats (e.g., Bloesch 1995; Hamilton and Mitchell 1996; Weyhenmeyer et al. 1997).

Comparisons of predicted benthic irradiance patterns with the subsaturation irradiance parameter of the dynamic photosynthesis model indicated that corals (specifically, *T. mesenterina*) at the study site fluctuate between states of potential light limitation and light stress (Fig. 6). A high rate of photoacclimation (15% per day) for the coral *T. mesenterina* (Anthony and Hoegh-Guldberg 2003) provided a conservative baseline for estimating the degree to which benthic irradiances fluctuate between suboptimal and supraoptimal levels. During extended periods of high turbidity and extensive clouds, particularly during November–March, gross photosynthesis can be reduced to <30% of average rates for periods of weeks. Depending on rates of respiration and other carbon losses, net productivity could be strongly reduced during such episodes, potentially affecting survivorship. For example, the energy balance of corals in both deep and shallow water might be strongly reduced or negative during high-turbidity events (Anthony and Fabricius 2000; Anthony et al. 2002). In deep, turbid-water habitats, light might limit net productivity most of the time, so that the timing of periods of enhanced growth versus energy deficit will depend primarily on the wind and wave regime (key factors causing resuspension) and secondarily on clouds and tides. Similar dependence of patterns of productivity on the transmission properties of the aquatic environment have been observed in other low-irradiance habitats, such as in Antarctic lakes (Moorhead et al. 1997), where periodic ice and snow accumulation decreases light transmission to the water column. Conversely, during episodes in which clear water, low cloud cover, and midday low tides coincide, high irradiances can lead to light stress and photoinhibition of the benthic primary producers, including corals (Brown et al. 1999; Hoegh-Guldberg and Jones 1999), macroalgae (Franklin et al. 1996), and sea grasses (Ralph and Burchett 1995). In photosymbiotic organisms, such as scleractinian corals (e.g., Dunne and Brown 2001), soft corals (Michalek-Wagner and Willis 2001), tridacnid clams (Buck et al. 2002), sponges (Fromont and Garson 1999), and sea anemones (Perez et al. 2001), extended periods of supraoptimal irradiances can lead to loss of symbionts (bleaching), which could adversely affect fecundity, growth, and survivorship (e.g., *see* review by Hoegh-Guldberg 1999). Contrary to the irradiance data, the 3–4-week and 8-week periodicities in predicted rates of photosynthesis were of almost equal importance. The most likely explanation is that the relative strength of the 8-week irradiance periodicity is reduced because of photoacclimation. Specifically, with changing irradiance regimes on a scale of months, the photosynthesis–irradiance curve parameters (review by Falkowski and Raven 1997) will shift accordingly and thus buffer changes in productivity. However,

on shorter timescales, photoacclimation is less significant because of limitations of its kinetics and because acclimation to frequent drops in irradiance are canceled out by acclimation to subsequent increases in irradiance (*see* Anthony and Hoegh-Guldberg 2003).

A likely atmospheric mechanism driving irradiance variation as a result of clouds and wave-induced resuspension of sediment is the Madden–Julian oscillation (MJO). The MJO is the dominant mode of intraseasonal variability in the behavior of large-scale pressure systems (which drive cloud and wind patterns) in the tropics, with timescales of 30–50 d (Madden and Julian 1994; Hendon et al. 1999; Wheeler and Kiladis 1999) and thus could be the forcing mechanism explaining the 8-week periodicity in the turbidity (via resuspension) and cloud patterns.

Irradiance variation in coastal, turbid-zone benthic habitats is strongly driven by wind-induced resuspension, and the contribution from turbidity to the irradiance variation increases with depth. Accordingly, the irradiance variation in subtidal, turbid-zone habitats can be more than an order of magnitude greater than the irradiance variation in surface waters or in offshore, clear-water benthic habitats. The outputs of the dynamic photosynthesis model for the coral *T. mesenterina* suggested that benthic primary producers at the turbid-water site alternate between periods of potential light limitation (energy deficiency) and light stress (photoinhibition).

Intraseasonal patterns in clouds and suspended solids (the latter driven mainly by winds) showed strong 8-week periodicities and weaker 3–4-week periodicities. Tides produced a distinct 2-week periodicity in the irradiance pattern but were of lower magnitude than the 3–4 and 8-week periodicities. The 8-week periodicity reflects the temporal activity pattern of large-scale pressure systems in the tropics (Madden–Julian atmospheric oscillation).

References

ALLEN, P. A. 1997. Earth surface processes. Blackwell Sciences.

ANTHONY, K. R. N., AND K. E. FABRICIUS. 2000. Shifting roles of heterotrophy and autotrophy in coral energetics under varying turbidity. J. Exp. Mar. Biol. Ecol. **252:** 221–253.

———, AND O. HOEGH-GULDBERG. 2003. Kinetics of photoacclimation in corals. Oecologia **134:** 23–31.

———, S. R. CONNOLLY, AND B. L. WILLIS. 2002. Comparative analysis of tissue and skeletal growth in corals. Limnol. Oceanogr. **47:** 1417–1429.

AUSTIN, R. W. 1974. The remote sensing of spectral radiance from below the ocean surface, p. 317–344. In N. G. Jerlov and E. S. Nielsen [eds.], Optical aspects of oceanography. Academic.

AUSTRALIAN BUREAU OF METEOROLOGY. 1995. Climatic averages of Australia. Commonwealth Bureau of Meteorology, Department of Environment, Australian Government Publishing Service.

BARNES, D. J., AND B. E. CHALKER. 1990. Calcification and photosynthesis in reef-building corals and algae, p. 109–131. *In* Z. Dubinsky [ed.], Ecosystems of the world: Coral reefs. Elsevier.

BLOESCH, J. 1995. Mechanisms, measurement and importance of sediment resuspension in lakes. Mar. Freshw. Res. **46:** 295–304.

BLOOMFIELD, P. 1976. Fourier analysis of time series: An introduction. Wiley.

BRODIE, J. L., M. J. FURNAS, A. D. L. STEVEN, L. A. TROTT, F. PANTUS, AND M. WRIGHT. 1997. Monitoring chlorophyll in the Great Barrier Reef lagoon: Trends and variability, p. 797–802. *In* 8th International Coral Reef Symposium, Panama. V. 1. Smithsonian Tropical Research Institute, Balboa.

BROWN, B. E., I. AMBARSARI, M. E. WARNER, W. K. FITT, R. P. DUNNE, S. W. GIBB, AND D. G. CUMMINGS. 1999. Diurnal changes in photochemical efficiency and xanthophyll concentrations in shallow water reef corals: Evidence for photoinhibition and photoprotection. Coral Reefs 18: 99–105.

BUCK, B. H., H. ROSENTHAL, AND U. SAINT-PAUL. 2002. Effect of increased irradiance and thermal stress on the symbiosis of *Symbiodinium microadriaticum* and *Tridacna gigas.* Aquat. Living Resour. 15: 107–117.

CULLEN, J. J., AND M. R. LEWIS. 1988. The kinetics of algal photoadaptation in the context of vertical mixing. J. Plankton Res. 10: 1039–1063.

DEPARTMENT OF ENVIRONMENT. 1997. Wave data recording program, Townsville region, 1975–1997. Queensland Government.

DUNNE, R. P., AND B. E. BROWN. 2001. The influence of solar radiation on bleaching of shallow water reef corals in the Andaman Sea, 1993–1998. Coral Reefs 20: 201–210.

DUNTON, K. 1994. Seasonal growth and biomass of the subtropical seagrass *Halodule wrightii* in relation to continuous measurements of underwater irradiance. Mar. Biol. 120: 479–489.

FALKOWSKI, P. G., AND J. A. RAVEN. 1997. Aquatic photosynthesis. Blackwell Science.

FRANKLIN, L. A., G. G. R. SEATON, C. E. LOVELOCK, AND A. W. D. LARKUM. 1996. Photoinhibition of photosynthesis on a coral reef. Plant Cell Environ. 19: 825–836.

FROMONT, J., AND M. GARSON. 1999. Sponge bleaching on the west and east coasts of Australia. Coral Reefs 18: 340.

GEIDER, R. J., H. L. MACINTYRE, AND T. M. KANA. 1996. A dynamic model of photoadaptation in phytoplankton. Limnol. Oceanogr. 41: 1–15.

HAMILTON, D. P., AND S. F. MITCHELL. 1996. An empirical model for sediment resuspension in shallow lakes. Hydrobiologia 317: 209–220.

HATCHER, B. G. 1990. Coral reef primary productivity: A hierarchy of pattern and process. Trends Ecol. Evol. 5: 149–155.

HENDON, H. H., C. ZHANG, AND J. D. GLICK. 1999. Interannual variation of the Madden–Julian oscillation during austral summer. J. Climate 12: 2538–2550.

HOEGH-GULDBERG, O. 1999. Climate change, coral bleaching and the future of the world's coral reefs. Mar. Freshw. Res. 50: 839–866.

———, AND R. J. JONES. 1999. Photoinhibition and photoprotection in symbiotic dinoflagellates from reef-building corals. Mar. Ecol. Prog. Ser. 183: 73–86.

KIRK, J. T. O. 1994. Light and photosynthesis in aquatic ecosystems, 2nd ed. Cambridge Univ. Press.

KLEYPAS, J. A. 1996. Coral reef development under naturally turbid conditions: Fringing reefs near Broad Sound, Australia. Coral Reefs 15: 153–167.

LARCOMBE, P., P. V. RIDD, A. PRYTZ, AND B. WILSON. 1995. Factors controlling suspended sediment on inner-shelf coral reefs, Townsville, Australia. Coral Reefs 14: 163–171.

MADDEN, R. A., AND P. R. JULIAN. 1994. Observations of the 40–50-day tropical oscillation—a review. Mon. Weather Rev. 122: 814–837.

MICHALEK-WAGNER, K., AND B. L. WILLIS. 2001. Impacts of bleaching on the soft coral *Lobophytum compactum.* I. Fecundity, fertilization and offspring viability. Coral Reefs 19: 231–239.

MOORHEAD, D. L., C. F. WOLF, AND R. A. WHARTON. 1997. Impact of light regimes on productivity patterns of benthic microbial mats in an Antarctic lake: A modeling study. Limnol. Oceanogr. 42: 1561–1569.

MUMBY, P. J., S. W. CHISHOLM, A. J. EDWARDS, S. ANDREFOUET, AND J. JAUBERT. 2001. Cloudy weather may have saved Society Island reef corals during the 1998 ENSO event. Mar. Ecol. Prog. Ser. 222: 209–216.

MUSLIM, I., AND G. JONES. 2003. The seasonal variation of dissolved nutrients, chlorophyll *a* and suspended sediments at Nelly Bay, Magnetic Island. Estuar. Coast. Shelf Sci. 57: 445–455.

ORPIN, A. R., P. V. RIDD, AND L. K. STEWART. 1999. Assessment of the relative importance of major sediment transport mechanisms in the central Great Barrier Reef lagoon. Aust. J. Earth Sci. 46: 883–896.

PEREZ, S. F., C. B. COOK, AND W. R. BROOKS. 2001. The role of symbiotic dinoflagellates in the temperature-induced bleaching response of the subtropical sea anemone *Aiptasia pallida.* J. Exp. Mar. Biol. Ecol. 256: 1–14.

POND, S., AND G. L. PICKARD. 1983. Introductory dynamical oceanography. Pergamon.

PREZELIN, B. 1992. Diel periodicity in phytoplankton productivity. Hydrobiologia 238: 1–35.

PRIESTLEY, M. B. 1981. Spectral analysis and time series. Academic.

RALPH, P. J., AND M. D. BURCHETT. 1995. Photosynthetic responses of the seagrass *Halophila ovalis* (R. Br.) Hook. f. to high irradiance stress, using chlorophyll *a* fluorescence. Aquat. Bot. 51: 55–66.

RIDD, P. V., AND P. LARCOMBE. 1994. Biofouling control for optical backscatter sediment sensors. Mar. Geol. 116: 255–258.

SERODIO, J., AND F. CATARINO. 2000. Modelling the primary productivity of intertidal microphytobenthos: Time scales of variability and effects of migratory rhythms. Mar. Ecol. Prog. Ser. 192: 13–30.

SHUMWAY, R. H. 1988. Applied statistical time series analysis. Prentice Hall.

VAN DUIN, E. H. S. 2001. Modeling underwater light climate in relation to sedimentation, resuspension, water quality and autotrophic growth. Hydrobiologia 444: 25–42.

WEYHENMEYER, G. A., L. HAKANSON, AND M. MEILI. 1997. A validated model for daily variations in the flux, origin, and distribution of settling particles within lakes. Limnol. Oceanogr. 42: 1517–1529.

WHEELER, M. C., AND G. N. KILADIS. 1999. Convectively coupled equatorial waves: Analysis of clouds and temperature in the wavenumber–frequency domain. J. Atmos. Sci. 56: 374–399.

WRIGHT, L. D. 1995. Morphodynamics of inner continental shelves. CRC.

WRIGHT, W. J. 1997. Tropical–extratropical cloudbands and Australian rainfall: I. Climatology. Int. J. Climatol. 17: 807–829.